


# A general theoretical description of the influence of isotropic chemical shift in dipolar recoupling experiments for solid-state NMR

## Journal Article

### Author(s):

Shankar, Ravi; [Ernst, Matthias](#) ; Madhu, Perunthiruthy K.; Vosegaard, Thomas; Nielsen, Niels C.; Nielsen, Anders B.

### Publication date:

2017-04-04

### Permanent link:

<https://doi.org/10.3929/ethz-b-000130295>

### Rights / license:

[In Copyright - Non-Commercial Use Permitted](#)

### Originally published in:

The Journal of Chemical Physics 146(13), <https://doi.org/10.1063/1.4979123>

# A General Theoretical Description of the Influence of Isotropic Chemical Shift in Dipolar Recoupling Experiments for Solid-State NMR

Ravi Shankar,<sup>1</sup> Matthias Ernst,<sup>2</sup> P. K. Madhu,<sup>3,4</sup> Thomas Vosegaard,<sup>1</sup> Niels Chr.

Nielsen<sup>1</sup> and Anders B. Nielsen,<sup>1\*</sup>

<sup>1</sup>Interdisciplinary Nanoscience Center (iNANO) and Department of Chemistry, Aarhus University,  
Gustav Wieds Vej 14, DK-8000 Aarhus C, Denmark.

<sup>2</sup>Physical Chemistry, ETH Zürich, Vladimir-Prelog-Weg 2, 8093 Zürich, Switzerland.

<sup>3</sup>Department of Chemical Sciences, Tata Institute of Fundamental Research, Homi Bhabha Road,  
Colaba, Mumbai 400 005, India.

<sup>4</sup>TIFR Centre for Interdisciplinary Sciences, TIFR, 21 Brundavan Colony, Narsingi, Hyderabad 500  
075, India.

\*Corresponding author: Anders Bodholt Nielsen (abn@inano.au.dk)

## Abstract

We present a general theoretical description that allows to describe the influence of isotropic chemical shift in homonuclear and heteronuclear dipolar recoupling experiments in magic-angle-spinning solid-state NMR. Through a transformation of the Hamiltonian into an interaction frame with the combined radio-frequency irradiation and the isotropic chemical shift, we determine an effective Hamiltonian to first order with respect to the relevant internal nuclear spin interactions. This unravels the essential resonance conditions for efficient dipolar recoupling. Furthermore, we propose how to handle situations where the resonance conditions are not exactly fulfilled. To verify the general theoretical description, we compare numerical simulations using a time-sliced time-dependent Hamiltonian with simulations using the calculated effective Hamiltonian for propagation. The comparisons are exemplified for the homonuclear dipolar recoupling experiments  $C7_2^1$  and POST- $C7_2^1$ .

KEYWORDS: Solid-state NMR spectroscopy, Dipolar recoupling experiments, Floquet theory.

Dipolar recoupling among spin-1/2 nuclei is routinely used in biological magic-angle-spinning (MAS) NMR to gain valuable insight into the atomic structure of complex systems [1-6]. To ensure efficient transfer of polarization between spins and accurate measurement of internuclear distances using dipolar couplings, a lot of effort has been devoted to develop efficient dipolar recoupling experiments for a variety of different nuclear spin systems and experimental conditions. This has led to numerous different dipolar recoupling sequences for either homo- or heteronuclear polarization transfer [7-9].

Most of the existing dipolar recoupling experiments have been developed using average Hamiltonian theory [10-13] (AHT) which has proven to be a powerful tool to analyze the action of challenging multi-pulse experiments in simple terms. An example of quite advanced experiments developed by such means are the symmetry-based pulse sequences [14-18]. Here, symmetry arguments have been used to develop selection rules to construct elegant pulse sequences with robust behaviors with respect to challenges such as rf inhomogeneity and large variations in isotropic chemical shifts while ensuring high polarization-transfer efficiency.

In particular, the influence of isotropic chemical shifts has been carefully analyzed since the perturbations from chemical-shift offsets in practical applications often exceeds the magnitude of the recoupled effective dipolar-coupling Hamiltonian. Thus, a basic need for dipolar recoupling pulse sequences is the ability to suppress the isotropic chemical shift for certain spectral regions. This can be highly challenging to fulfill for nuclear spin pairs with small dipolar couplings and large chemical-shift dispersions considering the practical limitations for the rf-field strengths. An example of improved compensation of isotropic chemical shift is the development of the so-called POST [15] element for the C-symmetry sequences. Based on higher-order average Hamiltonian calculations [12, 15], the POST element was proven to be better than a simple  $2\pi_x 2\pi_x$  element in terms of offset compensation [15].

Alternatively, one may consider the isotropic chemical shift and the rf field together. Such an approach was applied for the description of the Rotational Resonance Tickling ( $R^2T$ ) dipolar recoupling

experiment [19], the band-selective homonuclear CP (BSH-CP) experiment [20], and recently addressed for the so-called four-pulse recoupling (FPR) scheme [21]. The same method has also been used for homonuclear decoupling experiments with the Lee-Goldburg (LG) scheme [22] and the phase/frequency modulated (PMLG/FSLG) variants [23, 24]. In general, there are two main advantages of considering the isotropic chemical shift and the rf field together in the interaction-frame transformation: (i) The convergence of the series expansion is faster since the chemical-shift offset is often the biggest term in the spin-system Hamiltonian. This makes the theoretical description to determine the effective Hamiltonian simpler. (ii) The effective Hamiltonian will not contain any terms involving isotropic chemical shifts which will reduce the number of terms to calculate for the total effective Hamiltonian to a given order. However, such an approach has been used for relatively few experiments as this method will often break the requirement that the Hamiltonian has to be cyclic over the entire period of the pulse element – in particular when varying the isotropic chemical shift. To handle such problems, another approach is to use Floquet theory [25-27], where the effective Hamiltonian can be found even when the Hamiltonian involves several time dependencies which are not commensurate.

Knowledge concerning the effective time-independent Hamiltonian under any rf sequence provides certain advantages compared to performing numerical simulations based on time slicing of the time-dependent Hamiltonian. Besides the analytical insight which can be helpful to develop improved pulse schemes, the effective Hamiltonian found by analytical means can be determined independently for larger multi-spin systems by calculating and collecting the various terms separately. Combining such an approach with sparse matrix algorithms, as has been done for liquid-state NMR [28], may be useful to perform approximate simulations for larger spin systems in solids than is possible by direct numerical propagation procedures of the time-dependent Hamiltonian.

In this paper, we present a general concept to describe the influence of isotropic chemical shift under general amplitude and phase-modulated dipolar recoupling experiments. By transforming the Hamiltonian into an interaction frame using the effective field in a tilted frame, we present a general

formulation circumvents the requirement that the Hamiltonian has to be cyclic over the entire period of the pulse element. Additionally, it is proposed how to implement near-resonance conditions for finding the approximate effective Hamiltonian.

To describe the various elements of this new and general approach to pulse sequence analysis and design, we have split the theory section into four sub-sections to describe the proposed stepwise procedure. A repeating pulse element consisting of four pulses is used as an introductory example with the note that the pulse sequence itself does not have any applications. We then, as the second and more useful example, employ the theoretical framework to show how isotropic chemical shift influences the symmetry-based pulse sequences  $C7_2^1$  [14] and POST- $C7_2^1$  [15].

## Theory

For the theoretical description, we will consider two homonuclear coupled spin-1/2 nuclei,  $\hat{I}_1$  and  $\hat{I}_2$ , in the rotating frame (the Zeeman interaction frame). The time-dependent Hamiltonian includes the isotropic chemical shifts and the homonuclear dipole-dipole coupling under MAS and rf irradiation and is given by

$$\hat{H}(t) = \hat{H}_{I_q} + \hat{H}_{\text{rf}}(t) + \hat{H}_{I_1 I_2}(t) \quad (1)$$

with

$$\hat{H}_{\text{rf}}(t) = \sum_{q=1}^2 \omega_1(t) \left[ \hat{I}_{qx} \cos(\theta(t)) + \hat{I}_{qy} \sin(\theta(t)) \right] \quad (2)$$

$$\hat{H}_{I_q} = \sum_{q=1}^2 \omega_{I_q} \hat{I}_{qz} \quad (3)$$

$$\hat{H}_{I_1 I_2}(t) = \sum_{n=-2}^2 \omega_{I_1 I_2}^{(n)} e^{in\omega_r t} \left( 2\hat{I}_{1z}\hat{I}_{2z} - \hat{I}_{1x}\hat{I}_{2x} - \hat{I}_{1y}\hat{I}_{2y} \right) \quad (4)$$

where the angular frequencies  $\omega_1$  and  $\omega_2$  are the isotropic chemical shifts,  $\omega_{12}^D$  the dipolar coupling, and  $\omega_s$  the spinning frequency. The rf irradiation at a given time is described by the instantaneous

amplitude  $\omega_1(t)$  and phase  $\theta(t)$  in the transverse ( $x$ - $y$ ) plane. The anisotropic part of the chemical-shift Hamiltonian is not included in the interaction-frame transformation and will be described by higher-order terms in the effective Hamiltonian. The way to calculate these terms has recently been presented elsewhere [29, 30]. We note that the presented description is also valid for a heteronuclear dipolar coupling interaction with a truncation of the planar (terms containing the operators  $\hat{I}_x$  and  $\hat{I}_y$ ) operator terms of the dipolar Hamiltonian in Eq. (4).

Our goal is to calculate an approximate first-order effective time-independent Hamiltonian for the time-dependent Hamiltonian of Eq. (1) to characterize the time evolution of the nuclear spin systems. The sections below explain systematically step by step the theoretical process we propose. In section A), we show how to determine the effective axis of rotation and the corresponding effective frequency for the effective rf Hamiltonian represented by both Eq. (2) and Eq. (3). The effective axis of rotation and corresponding effective frequency are employed to determine the time dependence of a given single-spin operator in the tilted interaction frame of the effective rf-field Hamiltonian. This is presented in the supplementary material. In section B), we show the time dependencies for the dipolar coupling Hamiltonian in the effective rf interaction frame and present a general operator-based Floquet framework to determine the first-order effective Hamiltonian. In section C), we demonstrate how to handle situations where the resonance conditions are not exactly met. Finally, in section D), we show how to propagate with the determined effective Hamiltonian.

#### *A) The effective frequencies and axis of rotation for the effective rf Hamiltonian*

We transform Eq. (1) into an interaction frame containing both the rf Hamiltonian of Eq. (2) and the chemical-shift Hamiltonian of Eq. (3) for each of the two spins separately. This results in a double-rotating frame with, in general, different frequencies and different axes for the two spins. To do so, we



$$\hat{H}_{rf^{eff},q}(t) = \omega_{iso}^{I_q} \hat{I}_{qz} + \omega_1(t) [\hat{I}_{qx} \cos(\theta(t)) + \hat{I}_{qy} \sin(\theta(t))] \quad , \quad (5)$$

where  $\omega_{iso}^{I_q} = \omega_{I_q} - \omega_{rf}$  is the isotropic chemical-shift offset relative to the rf carrier frequency and  $\omega_{rf}$  denotes the carrier frequency while  $q$  refers to the **two** different nuclei and can take the values 1 or 2.

As an example we consider a pulse element consisting of four pulses which are repeated  $M$  times as presented in Fig. 1A. The time of the repeating pulse element can be defined by  $\tau_m$ , which for the present pulse example is given by  $\tau_m = 4\tau_p$ . This implies that  $\hat{H}_{rf^{eff},q}(t) = \hat{H}_{rf^{eff},q}(\tau_m + t)$  and the total mixing time for the experiment is  $M\tau_m$ .

**Figure 1**

Taking into account the isotropic chemical shift in the effective rf Hamiltonian will often break the periodicity of the pulse element (i.e., the effective rf Hamiltonian will cause an overall rotation over the time  $\tau_m$ ) and, therefore, introduce a nutation around an effective axis. The orientation of the effective axis of rotation for any pulse sequence can be **calculated in many ways, e.g., using** quaternions [31]. The effective axis for the effective rf Hamiltonian in Eq. (5) using the element in Fig. 1A is illustrated in the single-spin subspace by the red axis in Fig. 1B. The red dots represent the density operator as function of  $M$  **pulse sequence** elements and using the initial operator  $\hat{\rho}(0) = \hat{I}_{qz}$ . The effective **nutation** frequency  $\omega_{I_q}^{eff}$  tells how fast **the** single-spin operators **nutates** around the effective axis as a function of  $M\tau_m$ .

Equipped with the **direction and magnitude of the** effective axis of rotation, we define a new tilted single-spin subspace as shown in Fig. 1C. In this subspace, the red line corresponds to the effective axis of rotation for the complete pulse sequence and we define this axis as the effective z-axis



the  $\hat{I}_{qz}$  operator and transform it into  $\hat{I}_{qz}^{\text{eff}}$  with  $\hat{I}_{qz}^{\text{eff}} = R(\alpha_{\text{eff}}, \beta_{\text{eff}}, \gamma_{\text{eff}}) \hat{I}_{qz} R(\alpha_{\text{eff}}, \beta_{\text{eff}}, \gamma_{\text{eff}})^\dagger$  where the

same transformation is also used to rotate  $\hat{I}_{qx}$  into  $\hat{I}_{qx}^{\text{eff}}$  and  $\hat{I}_{qy}$  into  $\hat{I}_{qy}^{\text{eff}}$  (green lines in Fig. 1C).

Under conditions where the effective rf Hamiltonian leads to an overall cyclic rotation, the effective axis of rotation is undefined in the calculation. Under these conditions, no new effective coordinate system is found and the conventional single-spin subspace shown in black in Fig. 1C is used with  $\hat{I}_{qj}^{\text{eff}} = \hat{I}_{qj}$  where

$j$  can take the values  $x, y$ , or  $z$  and  $j^{\text{eff}}$  can take the values  $x^{\text{eff}}, y^{\text{eff}}$ , or  $z^{\text{eff}}$ .

As the effective rf-field Hamiltonian in Eq. (5) depends on the isotropic chemical-shift offset, we transform the dipolar-coupling Hamiltonian into the effective rf-field interaction frame for each spin operator separately given by

$$\tilde{\hat{I}}_{qj}(t) = \hat{U}^\dagger(t) \hat{I}_{qj} \hat{U}(t), \quad \hat{U}(t) = \hat{T} e^{-i \int_0^t \hat{H}_{\text{rf},q}^{\text{eff}}(t') dt'} \quad (6)$$

where  $j$  refers to the initial operator at  $t = 0$  and takes the index  $z$  for a heteronuclear dipolar coupling Hamiltonian and  $j$  is either  $x, y$ , and  $z$  for a homonuclear dipolar coupling Hamiltonian.  $\hat{T}$  denotes the Dyson time-ordering operator.

In order to conveniently express the time-dependencies of each single-spin operator in the effective rf-field interaction frame of Eq. (6), we employ the effective axis of rotation and the corresponding effective field frequency  $\omega_{1,1q}^{\text{eff}}$  as presented in the supplementary material.

### B) Calculating the effective Hamiltonian

In the effective rf field interaction frame, the overall Hamiltonian will only contain terms from the dipolar coupling (originating from Eq. (4)) given by

$$\tilde{\hat{H}}_{I_1 I_2}(t) = \sum_{n=-2}^2 \omega_{1,1_2}^{(n)} e^{in\omega_1 t} \left( 2\tilde{\hat{I}}_{1z}(t) \tilde{\hat{I}}_{2z}(t) - \tilde{\hat{I}}_{1x}(t) \tilde{\hat{I}}_{2x}(t) - \tilde{\hat{I}}_{1y}(t) \tilde{\hat{I}}_{2y}(t) \right) \quad (7)$$

the tilted frame of the effective field as

$$\tilde{\hat{I}}_{qj}(t) = c(t)_{q,x^{eff},j} \hat{I}_{qx^{eff}} + c(t)_{q,y^{eff},j} \hat{I}_{qy^{eff}} + c(t)_{q,z^{eff},j} \hat{I}_{qz^{eff}}, \quad (7a)$$

and the time-dependent coefficients are defined as discussed in the supplementary material. One can always rewrite Eq. (7) in a **compact form using** Fourier series given by

$$\tilde{\hat{H}}_{l_1 l_2}(t) = \sum_{n=-2}^2 \sum_{k_1=-\infty}^{\infty} \sum_{k_2=-\infty}^{\infty} \sum_{l_1} \sum_{l_2} \tilde{\hat{H}}_{l_1 l_2}^{(n,k_1,k_2,l_1,l_2)} e^{in\omega_m t} e^{ik_1\omega_m t} e^{ik_2\omega_m t} e^{il_1\omega_m^{eff} t} e^{il_2\omega_m^{eff} t}, \quad (8)$$

where  $l_1$  and  $l_2$  can only take the value zero when the effective rf field Hamiltonian in Eq. (5) is causing an overall cyclic rotation for the respective single-spin operators over period  $\tau_m$ . **This restriction can be understood by that the effective axis is not defined in this situation.**  $l_1$  and  $l_2$  can take the values 0 (for terms containing the operator  $\hat{I}_{qz^{eff}}$  along the effective axis) and  $\pm 1$  (for terms containing the operator  $\hat{I}_{qx^{eff}}$  and  $\hat{I}_{qy^{eff}}$ ) when the effective rf field Hamiltonian in Eq. (5) is not causing an overall cyclic rotation for the respectively single-spin operators over period  $\tau_m$ . The frequencies  $\omega_{qm}$  relate to the total time of the basic element by  $\omega_{qm} = 2\pi / \tau_{qm}$  which in the homonuclear case will fulfill  $\omega_{1m} = \omega_{2m}$ . However, this is not necessarily the case in heteronuclear experiments **where two different pulse elements can be employed on the two spins.** The Fourier components  $\tilde{\hat{H}}_{l_1 l_2}^{(n,k_1,k_2,l_1,l_2)}$  are given by

$$\tilde{\hat{H}}_{l_1 l_2}^{(n,k_1,k_2,0,0)} = \omega_{l_1 l_2}^{(n)} \sum_{j,j^{eff}} a_{k_1,j^{eff},j} a_{k_2,j^{eff},j} \hat{I}_{1j^{eff}} \hat{I}_{2j^{eff}}, \quad (9)$$

$$\tilde{\hat{H}}_{l_1 l_2}^{(n,k_1,k_2,0,\pm 1)} = \omega_{l_1 l_2}^{(n)} \sum_{j,j^{eff}} a_{k_1,j^{eff},j} \hat{I}_{1j^{eff}} \left[ \left( a_{k_2,x^{eff},j} \mp ia_{k_2,y^{eff},j} \right) \hat{I}_{2x^{eff}} + \left( a_{k_2,y,j} \pm ia_{k_2,x,j} \right) \hat{I}_{2y^{eff}} \right], \quad (10)$$

$$\tilde{\hat{H}}_{l_1 l_2}^{(n,k_1,k_2,\pm 1,0)} = \omega_{l_1 l_2}^{(n)} \sum_{j,j^{eff}} \left[ \left( a_{k_1,x^{eff},j} \mp ia_{k_1,y^{eff},j} \right) \hat{I}_{1x^{eff}} + \left( a_{k_1,y^{eff},j} \pm ia_{k_1,x^{eff},j} \right) \hat{I}_{1y^{eff}} \right] a_{k_2,j^{eff},j} \hat{I}_{2j^{eff}}, \quad (11)$$

This manuscript was accepted by J. Chem. Phys. Click [here](#) to see the version of record.

$$\tilde{H}_{I_1 I_2} = \omega_{I_1 I_2} \sum_j \prod_{q=1}^2 \left[ (a_{k_q, x^{eff}, j} + i a_{k_q, y^{eff}, j}) I_{q x^{eff}} + (a_{k_q, y^{eff}, j} - i a_{k_q, x^{eff}, j}) I_{q y^{eff}} \right], \quad (12)$$

with  $j$  taking the indices  $x$ ,  $y$ , or  $z$  for a homonuclear dipolar coupling interaction while  $j = z$  for a heteronuclear dipolar coupling interaction due to truncation of planar terms.  $j^{eff}$  takes the indices  $x^{eff}$ ,  $y^{eff}$  or  $z^{eff}$  when the effective rf field Hamiltonian in Eq. (5) is causing an overall cyclic rotation, respectively, for the single-spin operators and  $j^{eff} = z^{eff}$  if not. This implies that if both involved spins experience an overall cyclic rotation, it is only Eq. (9) that exists. If one of the involved spins experience an overall cyclic rotation and the other do not, then Eq. (9) and either Eq. (10) or Eq. (11) are active. Finally, if both spins do not experience an overall cyclic rotation then all Fourier components in Eqs. (9)-(12) exist. The complex Fourier coefficients  $a_{k_q, j^{eff}, j}$  are determined as presented in supplementary material. We note that the Fourier components in Eqs. (9-12) are represented in the tilted effective frame.

From Eq. (8), it can be seen that the dipolar-coupling Hamiltonian in the effective rf-field interaction frame contains terms with up to five fundamental frequencies given by  $e^{in\omega_1 t}$ ,  $e^{ik_q \omega_m t}$ , and  $e^{il_q \omega_{1,l_q}^{eff} t}$ . In Floquet theory, the number of fundamental frequencies can always be reduced if two frequencies are commensurate by describing them using the greatest common divisor. In our case, the total time of the basic elements are the same for homonuclear recoupling sequences with  $\omega_{1m} = \omega_{2m}$  and such sequences can always be described by collapsing the two Floquet dimensions into a single one. Such a description would require two-spin Fourier coefficients for the nine two-spin operators. For convenience and generality (heteronuclear recoupling), we only use the single-spin coefficients  $a_{k_q, j^{eff}, j}$  corresponding to single-spin operator transformation and use them to calculate effective Hamiltonians. In such a single-spin description, the calculation of the Fourier coefficients is simpler and more

The time-independent first-order dipolar Hamiltonian obtained from operator-based Floquet theory is given by the set of quintuples of integers that satisfy the resonance conditions [27, 30, 32]

$$n_0\omega_r + k_1\omega_{1m} + k_2\omega_{2m} + l_1\omega_{1,1}^{eff} + l_2\omega_{1,1,2}^{eff} = 0 \quad (13)$$

The effective time-independent dipolar coupling Hamiltonian at these resonance conditions can be found by collecting the terms for which Eq. (13) is fulfilled

$$\tilde{H}_{l_1 l_2}^{(1)} = \sum_{n_0, k_1, k_2, l_1, l_2} \tilde{H}_{l_1 l_2}^{(n_0, k_1, k_2, l_1, l_2)} \quad (14)$$

As the Fourier components  $\tilde{H}_{l_1 l_2}^{(n_0, k_1, k_2, l_1, l_2)}$  in Eq. (14) contain products of operators of the form  $\hat{I}_{qj}^{eff}$  according to the Eqs. (9) - (12), the effective dipolar coupling Hamiltonian can be represented in the effective zero/double quantum coordinate system as shown to the left in Fig. 2, spanned by the zero-quantum (ZQ)  $\hat{I}_{z^{eff}}^{ZQ} = \frac{1}{2}(\hat{I}_{1z^{eff}} - \hat{I}_{2z^{eff}})$ ,  $\hat{I}_{x^{eff}}^{ZQ} = \hat{I}_{1x^{eff}}\hat{I}_{2x^{eff}} + \hat{I}_{1y^{eff}}\hat{I}_{2y^{eff}}$  and  $\hat{I}_{y^{eff}}^{ZQ} = \hat{I}_{1y^{eff}}\hat{I}_{2x^{eff}} - \hat{I}_{1x^{eff}}\hat{I}_{2y^{eff}}$  or double-quantum (DQ)  $\hat{I}_{z^{eff}}^{DQ} = \frac{1}{2}(\hat{I}_{1z^{eff}} + \hat{I}_{2z^{eff}})$ ,  $\hat{I}_{x^{eff}}^{DQ} = \hat{I}_{1x^{eff}}\hat{I}_{2x^{eff}} - \hat{I}_{1y^{eff}}\hat{I}_{2y^{eff}}$  and  $\hat{I}_{y^{eff}}^{DQ} = \hat{I}_{1x^{eff}}\hat{I}_{2y^{eff}} + \hat{I}_{1y^{eff}}\hat{I}_{2x^{eff}}$  operators[33]. In the ZQ/DQ subspace, the effective dipolar coupling Hamiltonian is illustrated with the red arrows representing the direction and strength of the Hamiltonian for different crystal angles in Fig. 2.

**Figure 2**

**C) Calculating the effective Hamiltonian when resonance conditions are not exactly met**

Strictly speaking, Eq. (13) is only fulfilled at the exact resonance condition. But obviously the effective Hamiltonian is not zero when Eq. (13) is almost but not exactly fulfilled. Thus, we define a

threshold for the maximum deviation  $\Delta\omega_{\max}$ . From the resonance condition and the resonance conditions

are considered matched whenever the following condition is met

$$\left| n_0\omega_r + k_1\omega_{1m} + k_2\omega_{2m} + l_1\omega_{1,1_1}^{\text{eff}} + l_2\omega_{1,1_2}^{\text{eff}} \right| \leq \Delta\omega_{\max} \quad . \quad (15)$$

The size for the proposed  $\Delta\omega_{\max}$  is not well-defined but certain restrictions are required  $\Delta\omega_{\max}$  to ensure an approximately correct effective Hamiltonian. It is required that  $\Delta\omega_{\max}$  is smaller (more than a factor of 2) than the spinning frequency. Otherwise, Eq. (16) may be fulfilled multiple times which will lead to an overall wrong effective Hamiltonian in Eq. (14). Additionally, the maximum allowed value depends on the magnitude of  $\hat{I}_{qz}^{\text{eff}}$  the effective rf Hamiltonian in Eq. (5), i.e., the approximation is valid

for  $\Delta\omega_{\max} \ll \sqrt{\omega_1^2 + (\omega_{iso}^{1q})^2}$  .

In Eq. (15) we have artificially changed the allowed resonance conditions which will be summed to give the total effective dipolar-coupling Hamiltonian in Eq. (14). By allowing additional contributions to the effective dipolar coupling Hamiltonian, we have to add a correction term. In general, we define the correction term by  $\Delta\omega_{\text{near}} \leq \Delta\omega_{\max}$  that fulfills

$$\left| n_0\omega_r + k_1\omega_{1m} + k_2\omega_{2m} + l_1\omega_{1,1_1}^{\text{eff}} + l_2\omega_{1,1_2}^{\text{eff}} \right| = \Delta\omega_{\text{near}} \quad . \quad (16)$$

The correction term can be viewed as being compensated to either one of the two effective field frequencies  $\omega_{1,1_q}^{\text{eff}}$  as the single-spin operators cannot be differentiated in the DQ/ZQ subspace of the effective dipolar coupling Hamiltonian. Therefore, the correction to the effective dipolar coupling Hamiltonian should take the form of the operator that is along the corresponding effective axis  $\hat{I}_{qz}^{\text{eff}}$  . This is illustrated in Fig. 2B with a green arrow presented in the longitudinal direction in the ZQ/DQ subspace.

Looking at Eq. (16), the reason to define  $\Delta\omega_{\text{near}}$  is that it can take different values for different resonance conditions that may be fulfilled within the allowed range in Eq. (15). The effective time-

independent dipolar coupling Hamiltonian in Eq. (14) will be the sum of all allowed conditions in Eq. (16) and may therefore contain both DQ and ZQ terms. However, only one value for  $\Delta\omega_{near}$  can be

chosen for the total effective Hamiltonian which is given by

$$\bar{H}_{tot} = \bar{H}_{I_1 I_2}^{(1)} \pm \Delta\omega_{near} \hat{I}_{z^{eff}}^{ZQ/DQ}, \quad (17)$$

where the correction term can either be added or subtracted depending on the correction to the effective field frequency  $\omega_{1,1_q}^{eff}$ . This correction term can be viewed as a change of the effective rf field Hamiltonian in Eq. (5) by the amount  $\mp \Delta\omega_{near} \hat{I}_{z^{eff}}^{ZQ/DQ}$  and should in principle only take one value for one particular rf-interaction frame transformation. But when the effective dipolar coupling Hamiltonian contain both DQ and ZQ terms at different resonance conditions, we propose to collect all resonance terms even though it corresponds to different rf interaction frame transformations.

To select the size of  $\Delta\omega_{near}$  in Eq. (17), we compare the scaling factor of effective dipolar coupling Hamiltonian for all specific resonance conditions in Eq. (14). Then, we choose the value for  $\Delta\omega_{near}$  in Eq. (17) which gives the corresponding highest scaling factor.

#### D) Propagation with the effective Hamiltonian

Up to this point, we have determined the effective time-independent dipolar coupling Hamiltonian in the effective axis frame. In order to get the correct time evolution with the effective Hamiltonian in Eq. (17) compared to exact numerical simulations, it is required that the time step for the propagation time is given by the greatest common divisor (gcd) between the spinning frequency and modulation frequency,  $\tau_c = \frac{2\pi}{gcd(\omega_m, \omega_r)}$  which ensures that  $\tau_c$  is always a multiple of  $\tau_m$  and  $\tau_r$ . In case a continuous wave (CW) pulse scheme is analyzed where  $\tau_m$  is not defined, we set  $\tau_c = \frac{2\pi}{\omega_r}$ . Furthermore, the rotation caused by the effective field frequency  $\omega_{1,1_q}^{eff} \hat{I}_{qz^{eff}}$  has to be contained in the propagation.

Hence, at time  $\tau_c$  we do not have a cyclic time in the effective rf Hamiltonian interaction frame. This



averaging. Accordingly, the evolution of the density operator is given as

$$\hat{\rho}(\tau_{mix}) = e^{i \sum_{q=1,2} \omega_{1,q}^{eff} \hat{I}_{qz}^{eff} \tau_{mix}} e^{-i \bar{H}_{tot} \tau_{mix}} \hat{\rho}(0) e^{i \bar{H}_{tot} \tau_{mix}} e^{-i \sum_{q=1,2} \omega_{1,q}^{eff} \hat{I}_{qz}^{eff} \tau_{mix}}, \quad (18)$$

where  $\tau_{mix} = n \tau_c$  and  $n$  is an integer. It is noted that before calculating the evolution in Eq. (18), we transform back into the conventional rotating frame coordinate system by Euler angle rotations defined by taking the  $\hat{I}_{qz}^{eff}$  operator and rotate this into  $\hat{I}_{qz}$  with the opposite rotation direction as described in Subsection A) and given by  $\hat{I}_{qz} = R(\alpha_{eff}, \beta_{eff}, \gamma_{eff})^\dagger \hat{I}_{qz}^{eff} R(\alpha_{eff}, \beta_{eff}, \gamma_{eff})$ .

## Simulations and Discussion

We will in this section show that the proposed theoretical framework can explain how isotropic chemical shift influences the performance for dipolar recoupling sequences. We have chosen to analyze the symmetry-based dipolar recoupling sequences  $C7_2^1$  [14] and POST- $C7_2^1$  [15]. A schematic representation for the  $C7$  symmetry-based pulse sequence is presented in Fig. 3A. The sequences consist of a basic element that is repeated seven times with an incremental phase for each basic element by  $2\pi/7$ . The seven basic elements are timed such that the overall sequence takes two rotor periods and the rf field strength is constant throughout the sequence fulfilling  $\omega_1 = 7\omega_r$ . The basic element for the original  $C7_2^1$  sequence consists of two pulses which for the first element are phase-alternated between  $x$  and  $-x$  phase and where each pulse gives rise to an overall  $2\pi$ -rotation (lower left in Fig. 3A). The basic element for the POST- $C7_2^1$  sequence consists of three pulses that are phase-alternated between  $x$ ,  $-x$  and  $x$ , respectively. The flip angle for each pulse is adjusted such that the first pulse gives a  $\frac{1}{2}\pi$ -rotation, the second pulse a  $2\pi$ -rotation, and the third pulse a  $\frac{3}{2}\pi$ -rotation (lower right in Fig. 3A).

For the analysis of the sequences, we start by determining the effective axis of rotation  $\hat{I}_{qz}^{eff}$  for the entire pulse element (for both sequences, the period of the (POST-)C7 element is two rotor periods



which gives  $\omega_{1,m}^{eff}$  and  $\omega_{1,q}^{eff}$  as the effective field frequency of each spin  $q$ , respectively. To differentiate between  $DQ$  and  $ZQ$  resonance conditions, we always define the positive

operator  $\hat{I}_{qz}^{eff}$  whereas the scaling  $\omega_{1,q}^{eff}$  can be either positive or negative for the respective nuclei. In

Fig. 3B (for  $C7_2^1$ ) and 3C (for POST- $C7_2^1$ ), the sum of the two independent projections of the effective field Hamiltonian onto the x, y and z axis of the rotating frame coordinate system as a function of chemical-shift offset is presented. For the size, we have used the short notation given by

$$\left| \langle \hat{I}_{1j} | \omega_{1,1_1}^{eff} \hat{I}_{1z}^{eff} \rangle + \langle \hat{I}_{2j} | \omega_{1,1_2}^{eff} \hat{I}_{2z}^{eff} \rangle \right| / 2\pi = \left| \omega_{1,1_1}^{eff} + \omega_{1,1_2}^{eff} \right| / 2\pi .$$

The calculations represent conditions of 5.0 kHz MAS and rf field strength  $\omega_1 / 2\pi = 35$  kHz. In the cases presented, it turns out that the effective axis are either undefined (for cyclic rotation for the respectively single-spin operators) or almost along the conventional z-axis with operator  $\hat{I}_{qz}$  (for not cyclic rotation for the respectively single-spin operators).

The reason for summing and not subtracting the two effective field frequencies is that for both  $C7$  variants, the effective first-order dipolar coupling Hamiltonian is given by  $DQ$  operators [14, 15].

Hence, the sum of the effective field frequencies will interfere with the recoupled dipolar Hamiltonian with  $(\omega_{1,1_1}^{eff} + \omega_{1,1_2}^{eff}) \hat{I}_{z}^{DQ}$  in a similar way as presented in Fig. 2B and by Eq. (17).

### Figure 3

Looking at the z-component in Figs. 3B and 3C, it is obvious that the influence of isotropic chemical-shift offset for the POST element is significantly minimized relative to the original  $C7_2^1$  sequence. Over the calculated chemical-shift offset region, the absolute size  $\left| \omega_{1,1_1}^{eff} + \omega_{1,1_2}^{eff} \right| / 2\pi$  is below 140 Hz for the POST- $C7_2^1$  sequence whereas for the  $C7_2^1$  sequence the value is getting higher than 600 Hz.

We have determined the total effective Hamiltonian in Eq. (17) under the conditions given in Figs. 3B and 3C. This is done by initially calculating the effective dipolar Hamiltonian in Eq. (14) by

coupling Hamiltonian will contain both DQ and ZQ terms. As mentioned, we decide a threshold  $\Delta\omega_{\max}$

for which the resonance conditions are fulfilled. For the threshold, we have used the size of the dipolar coupling constant which in the following is set to  $b_{I_1 I_2} / 2\pi = 1.0$  kHz. The resonance conditions for both  $C7_2^1$  sequences must fulfill

$$\left| \left( n_0 + \frac{1}{2}k_1 + \frac{1}{2}k_2 \right) \omega_r + l_1 \omega_{1,1}^{\text{eff}} + l_2 \omega_{1,2}^{\text{eff}} \right| \leq \Delta\omega_{\max} \quad (19)$$

If the rf pulse is applied on-resonance ( $\nu_{iso}^1 = 0$  Hz) for both spins, the effective field frequencies  $\omega_{1,lq}^{\text{eff}}$  will be zero as the effective rf Hamiltonian in Eq. (5) is cyclic. In this case Eq. (17) will only be fulfilled when  $n_0 + \frac{1}{2}k_1 + \frac{1}{2}k_2 = 0$ . The values for  $k_1$  and  $k_2$  can be any integer number according to Eq. (8) but for practical reasons, we also set a threshold for largest absolute allowed values for these. We have defined the threshold by the size of the corresponding Fourier coefficients,  $a_{k_q, j^{\text{eff}}, j}$ . We have only allowed values for  $k_1$  and  $k_2$  for which  $a_{k_q, j^{\text{eff}}, j} \geq 10^{-3}$ . This threshold gives values for  $k_1$  and  $k_2$  up to  $\pm 25$  for the analyzed sequences. This sum of resonance conditions can be avoided (as discussed in the theory section), by combining dimensions with commensurate frequencies, i.e., in our case by combining the two frequencies  $\omega_{1m} = \omega_{2m}$ . This will automatically reduce the number of resonance conditions, but as mentioned, new Fourier coefficients need to be calculated.

At this point, it is easy to see that the total effective Hamiltonian in Eq. (17) is given by

$$\bar{H}_{tot} = \bar{H}_{I_1 I_2}^{(1)} = \sum_{n_0 \pm \frac{1}{2}k_1 \pm \frac{1}{2}k_2 = 0} \tilde{H}_{I_1 I_2}^{(n_0, k_1, k_2, 0, 0)} \quad (20)$$

When the rf pulse is applied off-resonance ( $\nu_{iso}^1 \neq 0$  Hz) for both spins, the effective field frequencies  $\omega_{1,lq}^{\text{eff}}$  will be finite and the effective rf Hamiltonians in Eq. (5) are not cyclic for the

resonance conditions. However, the scaling of the effective dipolar coupling Hamiltonian is much larger

for the DQ than for ZQ resonance conditions implying that  $\Delta\omega_{near} = |\omega_{1,l_1}^{eff} + \omega_{1,l_2}^{eff}|$  as presented in Figs. 3B

and 3C. It is also seen that  $|\omega_{1,l_1}^{eff} + \omega_{1,l_2}^{eff}| < \Delta\omega_{max} < \omega_r$  over the entire offset grid. These considerations

imply that the total effective Hamiltonian in Eq. (17) is given by

$$\bar{H}_{tot} = \sum_{n_0 \pm \frac{1}{2} k_1 \pm \frac{1}{2} k_2 = 0} \sum_{l_1, l_2 = -1}^1 \tilde{H}_{l_1 l_2}^{(n_0, k_1, k_2, l_1, l_2)} + \Delta\omega_{near} \hat{I}_z^{DQ} \quad (21)$$

If the rf pulse is applied off-resonance ( $\nu_{iso}^1 \neq 0$  Hz) for spin  $\hat{I}_1$  and on-resonance ( $\nu_{iso}^2 = 0$  Hz) for spin

$\hat{I}_2$  or visa versa, then the expression for the total effective Hamiltonian is given by Eq. (21) but  $l_2$  is

limited to only taking the value zero.

**Figure 4**

To verify if the calculated total effective time-independent Hamiltonian is correct, we compare

in Fig. 4 the propagation under the effective Hamiltonian with the direct-propagation numerical

SIMPSON simulations [34, 35]. In Figs. 4A and 4C, the simulated transfer efficiencies are shown for a

two-spin system as function of chemical-shift offset for both the original  $C7_2^1$  sequence (Fig. 4A) and

for POST- $C7_2^1$  sequence (Fig. 4C). The simulations were performed using the calculated effective

Hamiltonian and propagating according to Eq. (24) with a total mixing time of 3.2 ms ( $M=8$ ). Powder

averaging using 11  $\gamma_{CR}$  and 320  $\alpha_{CR}, \beta_{CR}$  REPULSION [36] crystallite angles were used with CR

denoting the transformation from the crystal axis frame to the rotor axis frame. By comparing Figs. 3B

with 4A as well as Figs. 3C with 4C, it can be seen that the overall transfer performance is highly

dependent on the effective field frequencies  $\omega_{1,l_q}^{eff}$ . This implies that the information content in the

effective axes and the effective field frequencies can be used to judge the transfer efficiencies as

function of chemical shift offset. Thus, minimizing variations in the effective field frequencies by using optimization procedures on quaternions may potentially be used to compensate for large chemical-shift variations. This is due to the fact that the resonance conditions are dependent on only up to two frequencies for each spin ( $\omega_m$  and  $\omega_{1,1q}^{eff}$ ) where only  $\omega_{1,1q}^{eff}$  changes when the offset is varied. Also, the calculation of  $\omega_{1,1q}^{eff}$  is much faster than performing a full direct propagation using the time-dependent Hamiltonian in Eq. (1).

In Figs. 4B and 4D, we have simulated the transfer efficiencies by direct-propagation using the numerical SIMPSON software package. The results are presented using the same settings as in Fig. 4A and 4C, respectively. By comparing the simulations in Fig. 4A with 4B and Fig. 4C with 4D, it can be seen that the proposed theoretical model is indeed representing the full spin-dynamics with greater the 99.5% accuracy. This illustrates that the determined first-order effective Hamiltonian found by the proposed theoretical description mimics the total time-dependent Hamiltonian in Eq. (1) to a really good approximation.

## Conclusions

In conclusion, we have presented a general theoretical description of how to handle isotropic chemical shift effects for dipolar recoupling experiments under magic-angle-spinning. By considering the isotropic chemical shift and the rf field together, the influence of chemical shift offset can directly be ascribed to a change in the dipolar resonance conditions for the first-order effective Hamiltonian. Additionally, we have shown that the low transfer efficiencies encountered under near-resonance conditions can be explained by an effective field along the effective axis in the related zero/double-quantum subspace. We have verified the proposed model and shown that the found first-order effective Hamiltonian for two versions of the symmetry-based pulse sequence  $C7_2^1$  gives same numerical results as found by numerical simulations using the SIMPSON software package. From the proposed description, we have shown that by representing the time-dependencies of single-spin operators with up to two frequencies for each spin ( $\omega_m$  and  $\omega_{1,1q}^{eff}$ ), we can obtain useful information to judge the overall

performance of this pulse sequence. Maly et al. show that only the  $\nu$  changes, when the offset is varied and affects the transfer efficiency. This insight may be exploited for faster optimizations for better offset compensation.

### Supplementary Material

See supplementary material for details on how to determine the time-dependency of a given single-spin operator in the interaction frame of the effective rf field Hamiltonian.

### Acknowledgments

We would like to thank support from the Danish Council for Independent Research (DFF-4090-00223), the Danish National Research Foundation (DNRF 0059), the Swiss National Science Foundation (Grants 200020\_146757 and 200020\_159797), the Danish Ministry of Higher Education and Science (AU-2010-612-181).



- [1] R. G. Griffin, *Dipolar recoupling in MAS spectra of biological solids*, *Nature structural biology* **5**, 508-512 (1998).
- [2] A. Loquet, N. G. Sgourakis, R. Gupta, K. Giller, D. Riedel, C. Goosmann, C. Griesinger, M. Kolbe, D. Baker, S. Becker, and A. Lange, *Atomic model of the type III secretion system needle*, *Nature* **486**, 276-279 (2012).
- [3] G. Comellas, and C. M. Rienstra, *Protein Structure Determination by Magic-Angle Spinning Solid-State NMR, and Insights into the Formation, Structure, and Stability of Amyloid Fibrils*, *Annual Review of Biophysics* **42**, 515-536 (2013).
- [4] M. T. Colvin, R. Silvers, Q. Z. Ni, T. V. Can, I. Sergeyev, M. Rosay, K. j. Donovan, B. Michael, J. Wall, S. Linse, and R. G. Griffin, *Atomic Resolution Structure of Monomorphic A $\beta$ 42 Amyloid Fibrils*, *Journal of the American Chemical Society* **138**, 9663-9674 (2016).
- [5] M. A. Wälti, F. Ravotti, H. Arai, C. G. Glabe, A. Böckmann, P. Güntert, B. H. Meier, and R. Riek, *Atomic-resolution structure of a disease-relevant A $\beta$  (1-42) amyloid fibril*, *Proceedings of the National Academy of Sciences* **113**, E5976-E4984 (2016).
- [6] J. T. Nielsen, N. V. Kulminkaya, M. Bjerring, J. M. Linnanto, M. Rätsep, M. Ø. Pedersen, P. H. Lambrev, M. Dorogi, G. Garab, K. Thomsen, C. Jegerschöld, N. Frigaard, M. Lindahl, and N. C. Nielsen, *In situ high-resolution structure of the baseplate antenna complex in *Chlorobaculum tepidum**, *Nature Communications* **7**, 12454 (2016).
- [7] V. Ladizhansky, *Homonuclear dipolar recoupling techniques for structure determination in uniformly  $^{13}\text{C}$ -labeled proteins*, *Solid State Nuclear Magnetic Resonance* **36**, 119-128 (2009).
- [8] N. C. Nielsen, L. A. Strassø, and A. B. Nielsen, *Dipolar Recoupling*, *Topics in Current Chemistry* **306**, 1-47 (2012).
- [9] G. D. Paëpe, *Dipolar Recoupling in Magic Angle Spinning Solid-State Nuclear Magnetic Resonance*, *Annual Review of Physical Chemistry* **63**, 661-684 (2012).
- [10] U. Haeberlen, and J. S. Waugh, *Coherent Averaging Effects in Magnetic Resonance*, *Physical Review* **175**, 453-467 (1968).
- [11] U. Haeberlen, *High resolution NMR in solids. Selective averaging*, Academic Press, New York (1976).
- [12] M. Mehring, *Principles of High Resolution NMR in Solids*, (Springer-Verlag, New York, 1983).
- [13] M. Hohwy, and N. C. Nielsen, *Systematic design and evaluation of multiple-pulse experiments in nuclear magnetic resonance spectroscopy using a semi-continuous Baker-Campbell-Hausdorff expansion*, *The Journal of Chemical Physics* **109**, 3780-3791 (1998).
- [14] Y. K. Lee, N. D. Kurur, M. Helmle, O. G. Johannessen, N. C. Nielsen, and M. H. Levitt, *Efficient Dipolar Recoupling in the Nmr of Rotating Solids - a Sevenfold Symmetrical Radiofrequency Pulse Sequence*, *Chemical Physics Letters* **242**, 304-309 (1995).
- [15] M. Hohwy, H. J. Jakobsen, M. Eden, M. H. Levitt, and N. C. Nielsen, *Broadband dipolar recoupling in the nuclear magnetic resonance of rotating solids: A compensated C7 pulse sequence*, *The Journal of Chemical Physics* **108**, 2686-2694 (1998).
- [16] A. Brinkmann, and M. H. Levitt, *Symmetry principles in the nuclear magnetic resonance of spinning solids: Heteronuclear recoupling by generalized Hartmann-Hahn sequences*, *The Journal of Chemical Physics* **115**, 357-384 (2001).
- [17] M. Edén, *Advances in Symmetry-Based Pulse Sequences in Magic-Angle Spinning Solid-State NMR*, in *eMagRes* (John Wiley & Sons, Ltd, 2007).
- [18] M. H. Levitt, *Symmetry in the design of NMR multiple-pulse sequences*, *The Journal of Chemical Physics* **128**, 052205 (2008).

- [19] P. R. Costa, B. Q. Sun, and R. G. Griffin, *Rotational resonance tickling: Accurate internuclear distance measurement in solids*, Journal of the American Chemical Society **119**, 10821-10830 (1997).
- [20] V. Chevelkov, C. Shi, H. K. Fasshuber, S. Becker, and A. Lange, *Efficient band-selective homonuclear CO-CA cross-polarization in protonated proteins*, Journal of Biomolecular NMR **56**, 303-311 (2013).
- [21] N. Khaneja, and A. Kumar, *Four pulse recoupling*, Journal of Magnetic Resonance **272**, 158-165 (2016).
- [22] M. Lee, and W. I. Goldberg, *Nuclear-Magnetic-Resonance Line Narrowing by a Rotating rf Field*, Physical Review **140**, A1261-A1271 (1965).
- [23] A. Bielecki, A. C. Kolbert, and M. H. Levitt, *Frequency-switched pulse sequences: Homonuclear decoupling and dilute spin NMR in solids*, Chemical Physics Letters **155**, 341-346 (1989).
- [24] E. Vinogradov, P. K. Madhu, and S. Vega, *High-resolution proton solid-state NMR spectroscopy by phase-modulated Lee-Goldburg experiment*, Chemical Physics Letters **314**, 443-450 (1999).
- [25] J. H. Shirley, *Solution of the Schrödinger Equation with a Hamiltonian Periodic in Time*, Physical Review **138**, B979-B987 (1965).
- [26] M. Leskes, P. K. Madhu, and S. Vega, *Floquet theory in solid-state nuclear magnetic resonance*, Progress in Nuclear Magnetic Resonance Spectroscopy **57**, 345-380 (2010).
- [27] I. Scholz, J. D. van Beek, and M. Ernst, *Operator-based Floquet theory in solid-state NMR*, Solid State Nuclear Magnetic Resonance **37**, 39-59 (2010).
- [28] I. Kuprov, N. Wagner-Rundell, and P. J. Hore, *Polynomially scaling spin dynamics simulation algorithm based on adaptive state-space restriction*, Journal of Magnetic Resonance **189**, 241-250 (2007).
- [29] K. O. Tan, V. Agarwal, B. H. Meier, and M. Ernst, *A generalized theoretical framework for the description of spin decoupling in solid-state MAS NMR: Offset effect on decoupling performance*, The Journal of Chemical Physics **145**, 094201 (2016).
- [30] K. Basse, R. Shankar, M. Bjerring, T. Vosegaard, N. C. Nielsen, and A. B. Nielsen, *Handling the influence of chemical shift in amplitude-modulated heteronuclear dipolar recoupling solid-state NMR*, The Journal of Chemical Physics **145**, 094202 (2016).
- [31] B. Blümich, and H. W. Spiess, *Quaternions as a practical tool for the evaluation of composite rotations*, Journal of Magnetic Resonance (1969) **61**, 356-362 (1985).
- [32] A. B. Nielsen, K. O. Tan, R. Shankar, S. Penzel, R. Cadalbert, A. Samoson, B. H. Meier, and M. Ernst, *Theoretical description of RESPIRATION-CP*, Chemical Physics Letters **645**, 150-156 (2016).
- [33] S. Vega, *Fictitious spin-1/2 operator formalism for multiple quantum NMR*, The Journal of Chemical Physics **68**, 5518-5527 (1978).
- [34] M. Bak, J. T. Rasmussen, and N. C. Nielsen, *SIMPSON: A general simulation program for solid-state NMR spectroscopy*, Journal of Magnetic Resonance **147**, 296-330 (2000).
- [35] Z. Tošner, R. Andersen, B. Stevansson, M. Eden, N. C. Nielsen, and T. Vosegaard, *Computer-intensive simulation of solid-state NMR experiments using SIMPSON*, Journal of Magnetic Resonance **246**, 79-93 (2014).
- [36] M. Bak, and N. C. Nielsen, *A Novel Approach to Efficient Powder Averaging in Solid-State NMR*, Journal of Magnetic Resonance **125**, 132-139 (1997).



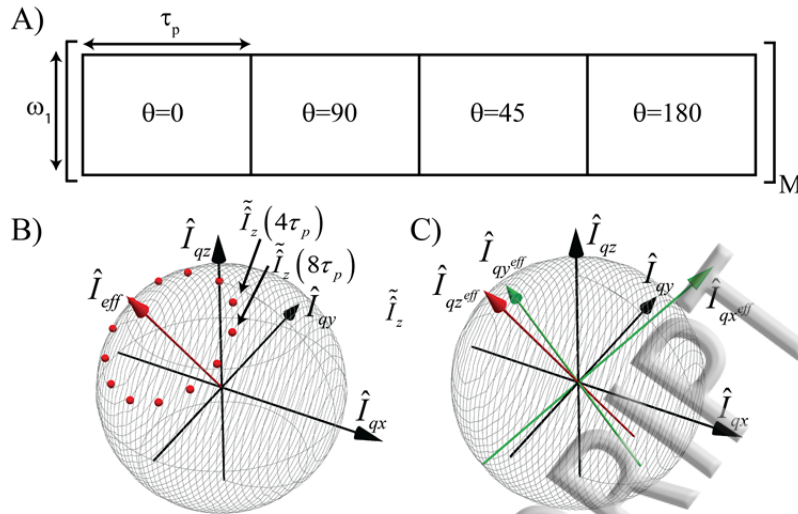


**Fig. 1.** (A) Schematic representation of a pulse element consisting of four pulses which is repeated  $M$  times. All pulses have the same field strength  $\omega_1$  and duration  $\tau_p$ . (B) Single-spin subspace for the time-evolution of interaction frame single spin operator  $\hat{I}_z(0) = \hat{I}_z$  using the conditions for the effective rf Hamiltonian given by  $\omega_{iso}^1 = 5.0$  kHz with  $\omega_1 / 2\pi = 9.0$  kHz and  $\tau_p = 100$   $\mu$ s. The red dots represent the density operator as function of  $M$  with the red axis illustrating the effective axis of rotation,  $\hat{I}_{eff}$ . (C) Shows the conventional single-spin subspace (black coordinate system) and the subspace (red and green lines) in which the effective axis of rotation for the pulse sequence is aligned with the new  $z$ -axis (red line).

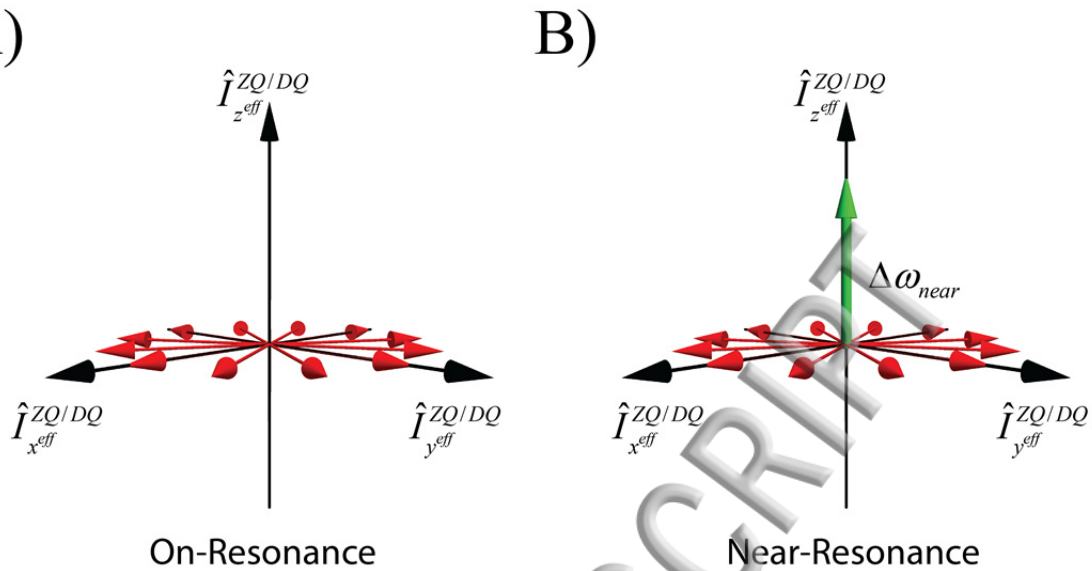


**Fig. 2.** The zero-/double-quantum subspace for the effective Hamiltonian in the effective axis coordinate system with the red arrows representing the strength of the effective dipolar coupling Hamiltonian for different crystal angles. In (A) the resonance condition in Eq. (13) is fulfilled whereas in (B) the resonance condition is only close to be fulfilled according to Eq. (15). The green arrow indicates the amount that is added to the effective Hamiltonian to fulfill a resonance condition. This term will be along the  $z$ -axis in the effective axis zero-/double-quantum subspace.

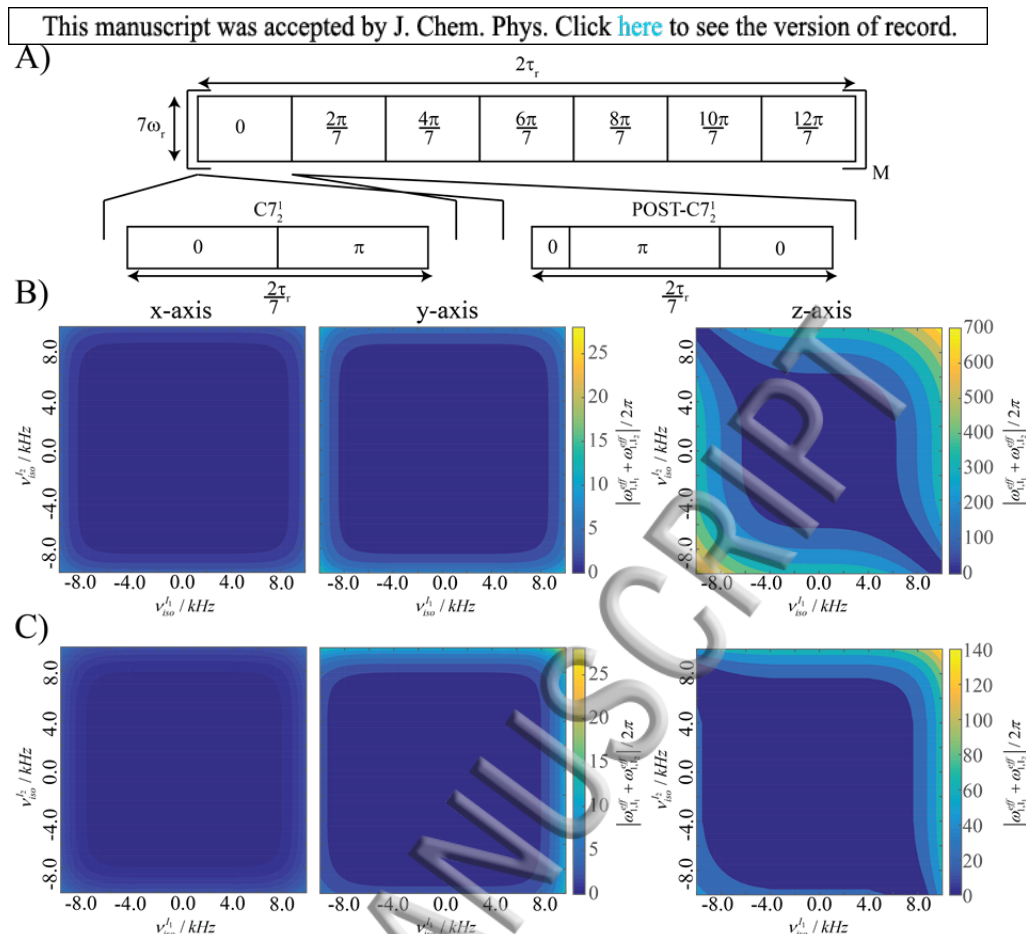


**Fig. 3.** (A) Schematic representation of the symmetry-based  $C7_2^1$  pulse sequence using either the original element consisting for the first element of two  $2\pi$  rotations with opposite phases (lower left) or the POST element consisting of a  $\frac{\pi}{2}$  rotation along the  $x$ -axis followed by  $2\pi$  rotation along  $-x$  and finally a  $\frac{3\pi}{2}$  rotation along the  $x$ -axis (lower right). (B) and (C) shows the magnitude of the sum of the effective frequencies  $|\omega_{1,1}^{eff} + \omega_{1,2}^{eff}|/2\pi$  for the conventional rotating frame coordinate system for  $x$ - (left),  $y$ - (middle) and  $z$ -axis (right) as a function of  $I_1$  and  $I_2$ -spin chemical shift offsets for  $C7_2^1$  pulse sequence (B) and the POST- $C7_2^1$  pulse sequence (C). The calculations were done for  $\omega_r/2\pi = 5.0$  kHz MAS with a rf field strength fulfilling  $\omega_1/2\pi = 35$  kHz.

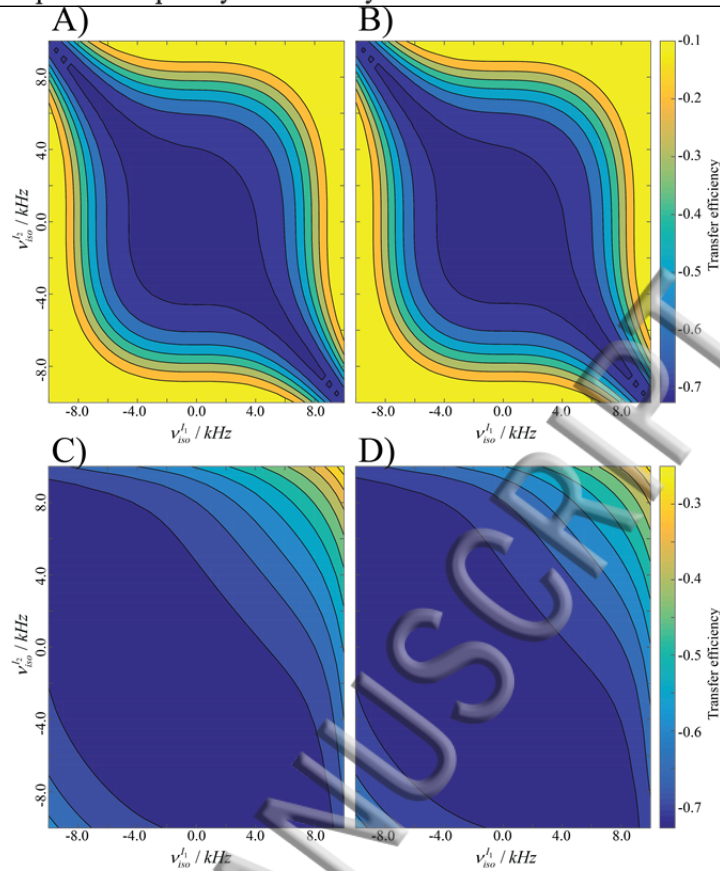
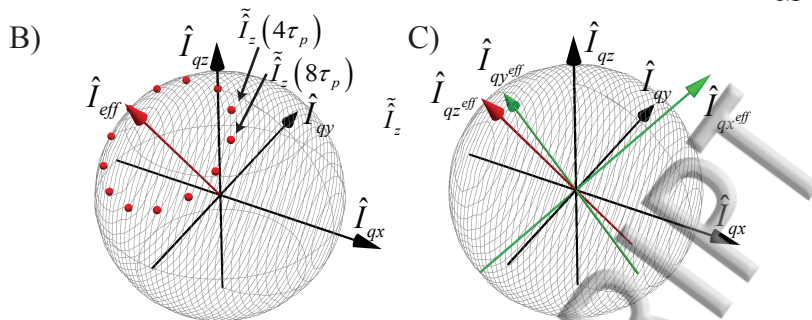
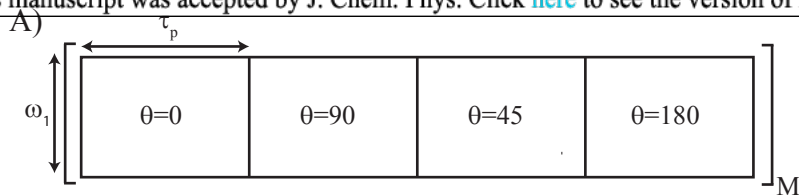
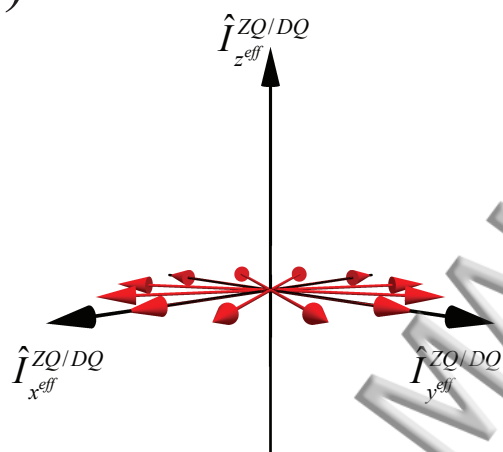


**Fig. 4.** Numerical simulations for the  $\hat{I}_{1z} \rightarrow \hat{I}_{2z}$  transfer efficiencies as a function of  $\hat{I}_1$  and  $\hat{I}_2$ -spin chemical shift offsets for the (A, B)  $C7_2^1$  and (C, D) and POST- $C7_2^1$  pulse sequences. For (A) and (C) the calculations were done using the effective Hamiltonian given in Eq. (22) and performing the propagation according to Eq. (23). For (B) and (D) the calculations were done using the SIMPSON software package [34, 35]. All simulations were done for  $\omega_r/2\pi = 5.0$  kHz MAS with a total mixing time set to 3.2 ms ( $M=8$ ) with rf field strength fulfilling  $\omega_1/2\pi = 35$  kHz. The dipolar coupling constant was set to  $b_{I_1I_2}/2\pi = 1.0$  kHz and powder averaging using 11  $\gamma_{CR}$  and 320  $\alpha_{CR}, \beta_{CR}$  REPULSION [36] crystallite angles with CR denoting the transformation from the crystal axis frame to the rotor axis frame.



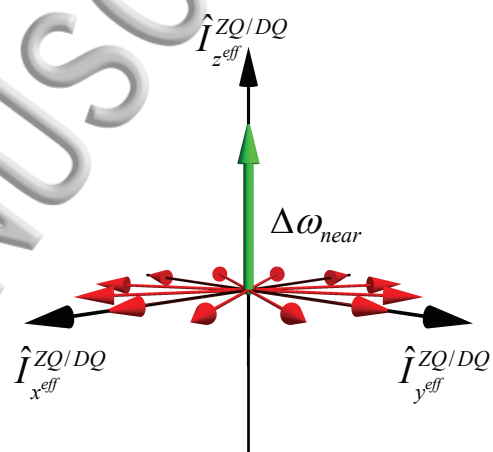
ACCEPTED MANUSCRIPT

A)



On-Resonance

B)



Near-Resonance

ACCEPTED MANUSCRIPT

